USGS
science for a changing world

Centimeter-Scale Surface Deformation Caused by the 2011 Mineral, Virginia, Earthquake Sequence at the Carter Farm Site—Subsidiary Structures with a Quaternary History

Open-File Report 2016–1134

U.S. Department of the Interior
U.S. Geological Survey

Centimeter-Scale Surface Deformation Caused by the 2011 Mineral, Virginia, Earthquake Sequence at the Carter Farm Site—Subsidiary Structures with a Quaternary History

By Richard W. Harrison, J. Stephen Schindler, Milan J. Pavich, J. Wright Horton, Jr., and Mark W. Carter

Open-File Report 2016–1134

U.S. Department of the Interior
U.S. Geological Survey

U.S. Department of the Interior
SALLY JEWELL, Secretary

U.S. Geological Survey
Suzette M. Kimball, Director

U.S. Geological Survey, Reston, Virginia: 2016

For more information on the USGS—the Federal source for science about the Earth, its natural and living resources, natural hazards, and the environment—visit http://www.usgs.gov or call 1–888–ASK–USGS.

For an overview of USGS information products, including maps, imagery, and publications, visit http://www.usgs.gov/pubprod/.

Suggested citation:
Harrison, R.W., Schindler, J.S., Pavich, M.J., Horton, J.W., Jr., and Carter, M.W., 2016, Centimeter-scale surface deformation caused by the 2011 Mineral, Virginia, earthquake sequence at the Carter farm site—Subsidiary structures with a Quaternary history: U.S. Geological Survey Open-File Report 2016–1134, 18 p., http://dx.doi.org/10.3133/ofr20161134.

ISSN 2331-1258 (online)

Contents

Figures

Conversion Factors

International System of Units to U.S. customary units

Multiply	By	To obtain
	Length	
centimeter (cm)	0.3937	inch (in.)
millimeter (mm)	0.03937	inch (in.)
meter (m)	3.281	foot (ft)
kilometer (km)	0.6214	mile (mi)

U.S. customary units to International System of Units

Multiply	By	To obtain
	Length	
foot (ft)	0.3048	meter (m)

Centimeter-Scale Surface Deformation Caused by the 2011 Mineral, Virginia, Earthquake Sequence at the Carter Farm Site—Subsidiary Structures with a Quaternary History

By Richard W. Harrison, J. Stephen Schindler, Milan J. Pavich, J. Wright Horton, Jr., and Mark W. Carter

Abstract

Centimeter-scale ground-surface deformation was produced by the August 23, 2011, magnitude (M) 5.8 earthquake that occurred in Mineral, Virginia. Ground-surface deformation also resulted from the earthquake aftershock sequence. This deformation occurred along a linear northeast-trend near Pendleton, Virginia. It is approximately 10 kilometers (km) northeast of the M5.8 epicenter and near the northeastern periphery of the epicentral area as defined by aftershocks. The ground-surface deformation extends over a distance of approximately 1.4 km and consists of parallel, small-scale (a few centimeters (cm) in amplitude) linear ridges and swales. Individual ridge and swale features are discontinuous and vary in length across a zone that ranges from about 20 meters (m) to less than 5 m in width. At one location, three fence posts and adjoining rails were vertically misaligned. Approximately 5 cm of uplift on one post provides a maximum estimate of vertical change from pre-earthquake conditions along the ridge and swale features. There was no change in the alignment of fence posts, indicating that deformation was entirely vertical. A broad monoclinal flexure with approximately 1 m of relief was identified by transit survey across surface deformation at the Carter farm site. There, surface deformation overlies the Carter farm fault, which is a zone of brittle faulting and fracturing along quartz veins, striking N40°E and dipping approximately 75°SE. Brecciation and shearing along this fault is interpreted as Quaternary in age because it disrupts the modern B-soil horizon. However, deformation is confined to saprolitized schist of the Ordovician Quantico Formation and the lowermost portion of overlying residuum, and is absent in the uppermost residuum and colluvial layer at the ground surface. Because there is a lack of surface shearing and very low relief, landslide processes were not a causative mechanism for the surface deformation. Two possible tectonic models and one non-tectonic model are considered: (1) tectonic, monoclinal flexuring along the Carter farm fault, probably aseismic, (2) tectonic, monoclinal flexuring related to a shallow (1–3 km) cluster of aftershocks (M2 to M3) that occurred approximately 1 to 1.5 km to the east of Carter farm, and (3) non-tectonic, differential response to seismic shaking between more-rigid quartz veins and soft residuum-saprolite under vertical motions that were created by Rayleigh surface waves radiating away from the August 23, 2011, hypocenter and propagating along strike of the Carter farm fault. These processes are not considered mutually exclusive, and all three support brittle deformation on the Carter farm fault during the Quaternary. In addition, abandoned stream valleys and active stream piracy are consistent with long-term uplift in vicinity of the Carter farm fault.

Introduction: Resident-Reported Ground-Surface Deformation

Following a public meeting held by the U.S. Geological Survey (USGS) in Louisa County to provide information on the August 2011, magnitude (M) 5.8 earthquake, farm residents at 973 Willis Profit Road (figs. 1 and 2) contacted the USGS and reported land surface changes on their property. They attributed these changes to the initial M5.8 earthquake and subsequent aftershocks during the following few weeks. The initial USGS visit to the site in early October, 2011, found several linear, ripple-like ridges and swales that had cm-scale amplitudes and spacing of less than 1 m (figs. 3*A* and 3*B*). Also present were small (8–10 cm diameter) scattered holes (fig. 3*C*) suggestive of water venting. The report that these features developed at the time of the August 2011, earthquake sequence was substantiated by two other people familiar with the yard area. Attempts to mow the rippled farm land after the August 2011, earthquakes resulted in either high-centering of the residents' lawnmower or scrapping of higher ridges that bent the mower's blade; thus giving crude experimental evidence supporting a recent formation of the features at this location. A more extensive survey of the landsurface and interviews with other local residents surrounding Carter farm found no indication of the surface features extending to the south or southwest. However, extending N40°E from

Carter farm for a distance of approximately 1.4 km (labeled locations *A*, *B*, *C*, and *D* on fig. 2) there is a visible zone of surface deformation that residents report had formed during the 2011 earthquake sequence. The yard of the next inhabited property to northeast of Carter farm at 1175 Willis Profit Road (location *B* on fig. 2) contains ripple-like features similar to those at Carter farm that the resident reported were not present prior to the 2011 earthquake sequence. Also at this location, a relatively new east-to-west fence has three posts (set in concrete) and connecting rails conspicuously out of vertical alignment (fig. 3*D*). The resident reports that these changes occurred during the 2011 earthquake sequence. One post appears to be approximately 4 to 5 cm higher than it was prior to the seismic events. Open, cultivated fields between Carter farm and 1175 Willis Profit Road contain numerous ridge and swale features at the surface, but there is no knowledge of pre-earthquake conditions. Cultivated fields immediately northeast of 1175 Willis Profit Road also contain ridge and swale features, but again pre-2011 coniditions are unknown. Further to the northeast, residents at 1309 Willis Profit Road (location *C* on fig. 2) report that rainwater accumulates in puddles in their yard in different locations than it did prior to the August 2011, earthquake, suggesting probable ground disturbance. There are numerous N45°E-striking ripples similar to those at Carter farm running across the property, but the residents could not say if any were formed around the time of the earthquake. At the northeast end of the identified deformed zone (location *D* on fig. 2), there is a subtle N40°E-trending, northwest-facing scarp with as much as 1 m of relief. The residents there report that the scarp did exist before the August 2011, earthquake. However, a small mound formed in their driveway at the base of the scarp during the earthquake. This feature was large enough that it had to be removed by shoveling before they could exit their property. When the USGS first visited this property in November 2011, there were no visible remains of the mound.

The zone of surface deformation occurs on the northwest side of a northeast-elongated hill. Willis Profit Road follows the crest of this hill in this area. On the southeast side of this hill (southeast of Willis Profit Road) over a distance of about 0.75 km, there are numerous cm-scale ridge and swale features in open fields, as well as several topographic scarps and an elongated synform depression. All of these surficial landforms trend northeast-southwest, parallel to the features on the northwest side of the hill. Residents reported that the scarps existed prior to 2011 and that they were unaware of any recent change in the surface morphology. The synform depressions (dotted lines on fig. 2) are clearly old features and appears to be a paleo-valley system that has been abandoned and dissected. At the southeastern base of the elongated hill there are two prominent northeast-trending valleys in line with one another and separated by one of the synform depressions (see fig. 2). One of these valleys is occupied by a stream (labeled Indian Creek on fig. 2) that flows southwestward into South Anna River. The other valley has a stream that flows northeastward for a short distance into Little River and is actively pirating surface drainage from the South Anna tributary.

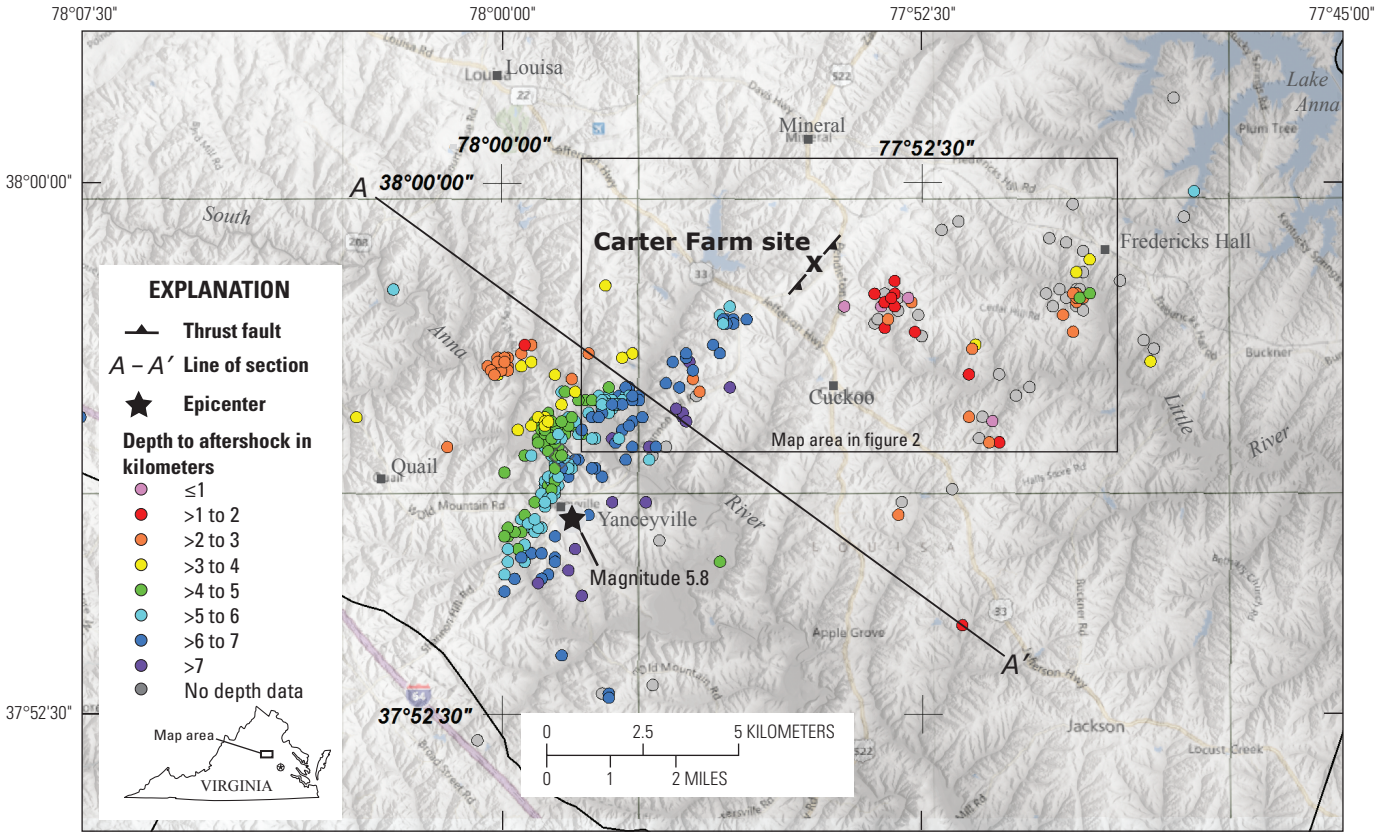

Modified from McNamara and others (2014) and Horton and others (2015)

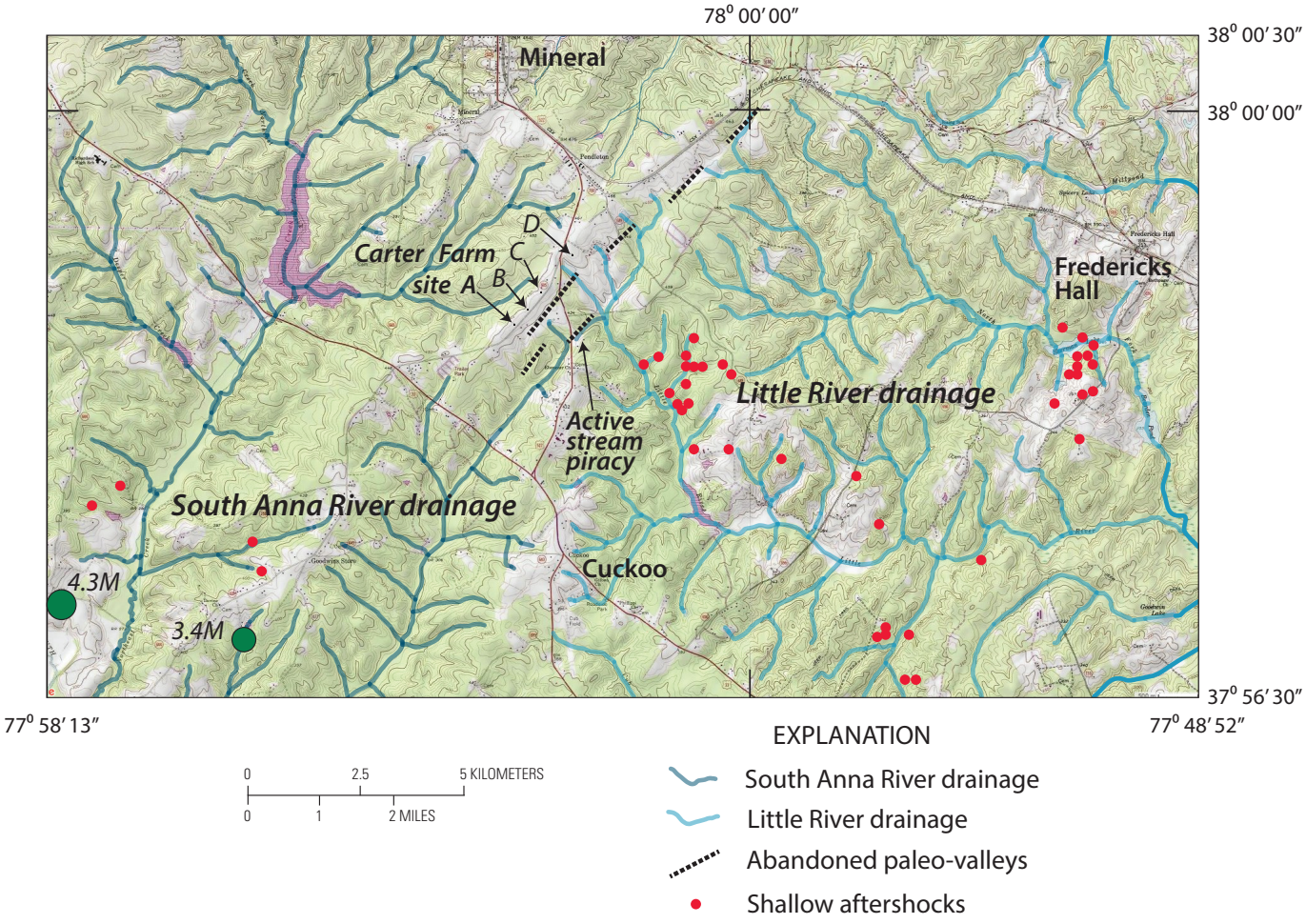

Figure 2. Map of area surrounding the Carter farm site showing aftershock locations following the August 23, 2011, magnitude 5.8 earthquake (2 km south of the southwest corner of this map). The map also shows the locations (*A*, *B*, *C*, and *D*) identified by residents as land surface changes, and later by the U.S. Geological Survey as sites of cm-scale surface deformation related to the August 2011, earthquake sequence. Location *A* is at 973 Willis Profit Road (on Carter farm); Location *B* and *C* are located at 1175 and 1309 Willis Profit Road, respectively; Location *D* is at 1832 Pendleton Road (Highway 522). Red circles are locations of earthquake aftershock epicenters recorded between August 23, 2011, and January 1, 2013, from the U.S. Geological Survey and McNamara (2014; electronic supplement table S1); these aftershocks are limited to those with magnitudes between 2 and 3, and are less than 2 km in depth. Two larger and deeper aftershocks (green circles in the southwest corner of the map) are also shown (the magnitude 4.3 (4.3M) at 5.5 km depth on August 24, 2011, and the magnitude 3.4 (3.4M) at 7.4 km depth on September 1, 2011). The black dotted lines are abandoned paleo-valleys (coincide with northeast-trending topographic synforms). One arrow points to the location of active stream piracy by headwaters of the Little River drainage (light-blue streams) and from the South Anna River drainage (dark-blue streams). The base map is a composite of four U.S. Geological Survey 1:24,000-scale topographic maps including: the Pendleton 7.5-minute map at the Carter farm site; bounded to the east by the Buckner 7.5-minute map; bounded to the northeast by the West Lake Anna 7.5-minute map; and bounded to the north by the Mineral 7.5-minute map.

Figure 1 (page 2). Map of area surrounding the epicenter of the August 23, 2011, magnitude 5.8 earthquake (black star) and the aftershock epicenters as of July 30, 2012 (colored circles); from MacNamara and others (2014) and from Horton and other (2015). Location of small-scale surface deformation along Willis Profit Road that is described in this report (shown with X), located about 10 km to the northeast of the magnitude 5.8 epicenter. The thrust fault symbol adjacent to the X represents a N40°E and approximately 75°SE attitude of the Carter farm fault discussed in this report.

Carter Farm Site Investigations

The Carter farm lies on the northwest side of a broad northeast-elongated ridge. This ridge has a 6.25 percent slope below the farm yard (50 feet (ft) difference in elevation over 800 ft distance from U.S. Geological Survey Pendleton 7.5-minute topographic map) and a 3.0 percent slope above the farm yard (approximately 12 ft elevation difference over a distance of 400 ft). Carter farm is underlain by the Ordovician Quantico Formation, comprised of staurolite-garnet-muscovite phyllite and schist (Marr, 2002). The Quantico Formation is Late Ordovician, based on paleontological data (Pavlides and others, 1980) and zircon U-Pb geochronology (Horton and others, 2010). Regionally, the Quantico Formation is mapped as a relatively narrow (2- to 3-km-wide), northeast-trending, structurally bound outcrop belt that extends for more than 70 km in the Virginia Piedmont province (Marr, 2002; Mixon and others, 2000). Rocks of the Quantico Formation occur in a tight synform, characterized by steeply dipping to vertical foliation (Mixon and others, 2000). The Quantico outcrop belt extends southwestward from the Carter farm into the aftershock epicentral area and beyond. More recent geologic mapping has resulted in the reinterpretion of many aspects of the aforementioned previous mapping (see fig. 1 of Burton and others, 2015).

The surface features that formed as a result of the 2011 earthquake sequence at Carter farm are low-amplitude (cm-scale), parallel to sub-parallel, linear ridges and swales (fig. 3*A* and *B*). Individual features vary in length and continuity; the most continuous features are between 10 and 20 m in length. Because the swales were better defined than the ridges in the field, the locations of the swales were surveyed by transit and are shown on figure 4. The swales consistently strike N40°E ±10° (figs. 4 and 5*A*). The longest and most prominent swale is on the eastern side of the deformed area and is on strike with one of the pre-existing northwest-facing topographic scarps. This swale is well expressed in the earthen floor of the gray barn where all four corner posts are tilted about 3 to 4° to the west. Unfortunately, there is no pre-earthquake baseline to compare this tilting to. The residents, however, report that the air space between the bottom of the siding on the barn and the ground surface increased noticeably along the southeast side of the barn, suggesting that the barn was affected by the earthquake.

A surveyed profile across the surface features (fig. 6) shows a low arch (1 m of relief over aprroximately 30 m of distance). The ridge and swale features modify the top of the low arch. The envelope defined by ridge crests and swale troughs is rather uniform in height (approximately 7–10 cm) and it shows a prominent break in slope at the crest of the low arch, near the western side of the gray barn. Assuming that the pre-earthquake profile along the same survey line of figure 6 was somewhere within the envelope, the deformation appears to have increased the surface area of the land surface, consistent with arching.

Two exploratory trenches (locations shown on fig. 4) were excavated across the deformed surface area at Carter farm. The south trench (fig. 7 diagrammatic log) was selected to minimize damage to the farmyard and yet still trench through a relatively densely deformed area. The north trench (fig. 8 diagrammatic log) was selected to cut through the pre-existing topographic scarps and to document continuity of subsurface geology identified in the south trench.

In an upward sequence, stratigraphic units in the Carter farm trenches are saprolitized schist of the Quantico Formation, residuum, and colluvium. Several quartz veins (figs. 9*A*, *B*, and *C*) cut the saprolite and are traceable into residuum as disintegrating masses that do not extend into the colluvial layer. Numerous red-clay-filled fractures (fig. 9*D*) cutting saprolite occur in both trenches, but only in the north trench there are thin (1–2 cm) brown, silty clay-filled fractures present that cut residuum and saprolite. Some, although rare, unfilled fractures occur in both trenches. Discontinuous deposits of more highly concentrated gravel occur locally at the base of colluvium and are thought to be either old tree-fall-root droppings or anthropogenic. Because they rest directly on dense, low porosity residuum, dewatering of these gravel concentrations (perched aquifer) is considered a probable source of the small (<5 cm-diameter) blow-hole-like surface depressions.

Saprolite of the Quantico Formation

The Quantico Formation lithology exposed in the Carter farm trenches consists of garnet-bearing quartz-muscovite schist that has been intensely to moderately decomposed to saprolite. It is soft and chemically altered, yet it still preserves its original lithologic fabric. One generation of well-developed schistosity is present that strikes N40°E ±10° and dips approximately 75° to the southeast (figs. 5*B*, 7, and 8). Adjacent to some quartz veins, (for example, at about the 13-m and 15-m lines on the south trench log (fig. 7), and at about the 20-m line on the north trench log (fig. 8)) foliations are rotated as much as 45° to east-west orientations in small (5–10 cm dimensions), fracture-bound fragments (these orientations are not shown on the foliation stereonet (fig. 5*B*)).

Saprolitized garnet-mica schist in the Carter farm trenches is crumbly and friable. Macroscopically, this medium-light-gray to grayish-red, crumbly saprolite is well foliated (schistose) and has a subtle lineation defined by microcrenulations on foliation surfaces. A fine-grained matrix containing white mica and graphite surrounds dusky red goethite pseudomorphs of euhedral garnet porphyroblasts up to 3 millimeters (mm) across. X-ray diffraction indicates that the saprolitized schist is now largely

Figure 3. Photos showing surface deformation at Carter farm (973 Willis Profit Road) following the August 23, 2011, magnitude 5.8 earthquake sequence. *A*, Photo along strike of the surface ridges and swales that formed during the earthquake sequence; the view is towards the southwest, and the white arrows are pointing at more prominent ridges. *B*, Photo looking across the same features towards the southeast in relation to the exploratory south trench; the white arrows are pointing at more prominent ridges. *C*, Photos of two separate holes, approximately 8 to 10 cm-diameter, that formed during the earthquake sequence. *D*, Deformed fence line at 1175 Willis Profit Road (location *B* in fig. 2); the fence runs approximately east to west (right to left) as viewed to the north; arrow above the post represents uplift of about 5 cm. *E*, Same deformed fence as in *D*, but viewed closer and towards the southwest.

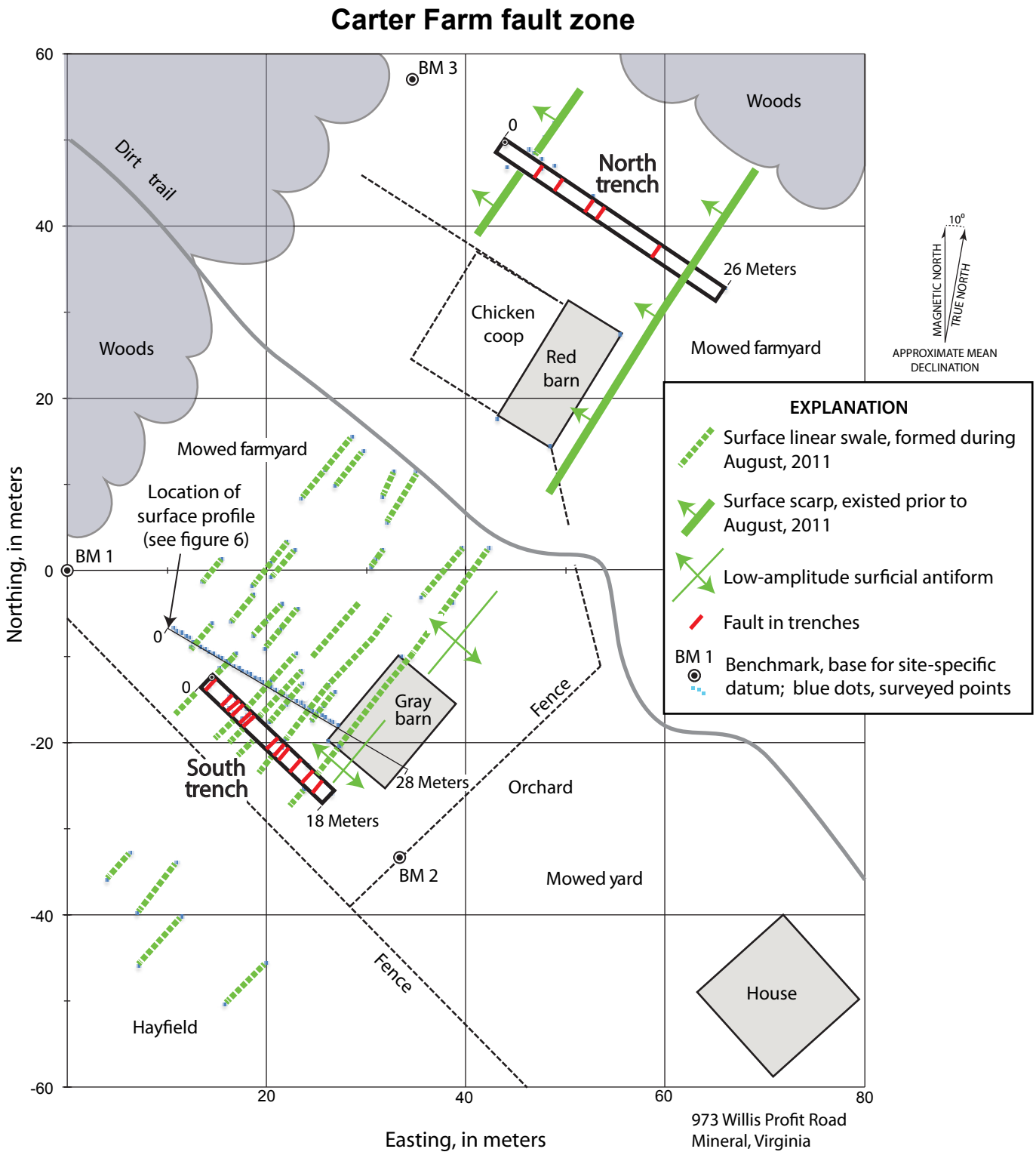

Figure 4. Site specific map of the Carter farm property (973 Willis Profit Road) showing various geomorphic surface features and the locations of exploratory trenches. The survey was carried out with a precision total station (Pentax); the grid system is in meters referenced to benchmarks (BM) and magnetic north; benchmark BM 1 is at geographic coordinates 39.97753°N, 77.90742°W, as determined by Wide Area Augmentation System (WAAS) corrected GPS (+/- 3 meters). Relative accuracy internal to the site specific grid is sub-centimeter, both horizontal and vertical. The map grid position relative to external geographic positions is limited by GPS errors.

composed of white mica (muscovite) and secondary minerals (notably kaolinite and goethite) attributed to chemical weathering. Petrographic analysis of thin sections indicates that the saprolitized schist consists of white mica (approximately 64 percent), goethite pseudomorphs after garnet (12–15 percent) and kaolinite pseudomorphs after tabular feldspar porphyroclasts. In addition, there are sparse remnants of less weathered plagioclase having albite twins (10–18 percent), opaque minerals (5–9 percent, including graphite), and tourmaline (1–2 percent). Trace minerals (<1 percent) include quartz inclusions in pseudomorphs after garnet. The goethite pseudomorphs after garnet porphyroblasts are euhedral to subhedral, range from less than 1 to 3 mm in diameter, have boxwork texture attributed to garnet dissolution during chemical weathering, and locally contain remnants of garnet. Tourmaline occurs as tiny (<1 mm) olive-green to yellow-green prismatic porphyroblasts parallel to mica foliation and is commonly also parallel to crenulation axes. In some kaolinite pseudomorphs after feldspar porphyroclasts, ghosts of cleavage planes separate intragranular micropores of weathered-out material. The graphite percentage is difficult to estimate but appears to be about 1 percent. Biotite was not observed, but porphyroclasts that may have formed by chemical weathering of biotite consist of non-pleochroic, colorless, phyllosilicate books having parallel extinction, locally bent cleavage, and accordion texture with secondary opaque oxides along cleavage surfaces. A thin section perpendicular to crenulation axes shows two foliations, which include (1) schistosity defined by white micas, and (2) crenulation cleavage that intersects the schistosity at angles of 11 to 28° and is axial planar to microcrenulations that fold the schistosity, confirming that microcrenulations observed macroscopically on foliation surfaces are intersection lineations.

Quartz Veins in Saprolite

Many quartz veins cut the Quantico Formation in both trenches. The veins are up to approximately 0.5 m wide and are strongly fractured, broken, and locally dislocated. Strike of the quartz veins generally follows the schistosity of N40°E ±10° dipping approximately 75°SE. Notable exceptions trend north to north-northwestward and are strongly discordant to schistosity (fig. 5*C*). At many locations where the quartz veins trend similar to schistosity, they cross cut foliation at a very acute angles. Non-clay-filled fractures occur at many places along the margins and within quartz. Red-clay-filled fractures cross cut and run along the margins of the quartz veins. Some red-clay-filled fractures adjacent to the quartz veins contain numerous fragments of angular granulated quartz. Vein-cutting, red-clay-filled fractures have a bi-modal, NNE and NNW strike, and dip moderately to the NE and NW (fig. 5*E*).

Slickenside striations occur at six locations along fractured margins of quartz veins (fig. 5*C*). At approximately the 6-m line on the south trench log (fig. 7) along the footwall of a quartz vein, slickenside striations were measured striking N50°E, dipping 78°SE, and raking 80°NE; this surface was on a red-clay-filled fracture containing quartz fragments. At about the 11-m line on the south trench log (fig. 7) on the hanging wall of a quartz vein, slickenside striations were measured striking N45°E, dipping 75°SE, and raking 78°SW. At about the 15-m line on the south trench log (fig. 7) on the footwall of a quartz vein, slickenside striations were measured striking N40°E, dipping 74°SE, and raking 90°. At approximately the 16.5-m line on the north trench log (fig. 8), slickenside striations striking N45°E, dipping 80°SE, and raking 90° were measured on the margin of a red-clay-filled fracture cutting through a quartz vein. At approximately the 20-m line on the north trench log (fig. 8), slickenside striations were measured raking 90° on a surface striking N40E and dipping 67°SE (measured on a non-clay-filled fracture that cross cuts and appears to offset a wide quartz vein).

Plan views of the quartz veins between the 10- and 15-m lines in the floor of the south trench (fig. 7 and figs. 9*A* and 9*B*) document a fractured fabric consisting of repeated sets of N10°E and N40 to 50°E orientations, producing common rhombohedral patterns that are elongated to northeast-southwest and shortened to the northwest-southeast. This strain is consistent with an overall northeast-southewest subhorizontal contractional stress.

Graphite occurs along the margins of five quartz veins between the 10- and 15-m lines on the south trench log (fig. 7). The mineral occurs as podiform bodies that are a few cm in width and elongated steeply down dip to the southeast, and as thin (<2 mm) seams along fractures located at the hanging wall and footwall margins of the veins.

The age of the quartz mineralization at the Carter farm is unknown, however, it is younger than the Late Ordovician Quantico Formation. The quartz mineralization age is also considered to be no younger than Jurassic, since that is the last time regional magmatism and potentially associated hydrothermal activity occurred. Petrographically, the quartz veins appear to lack a metamorphic foliation, and although in places they are slightly discordant to foliation, overall veining follows the metamorphic fabric (fig. 5). Vein mineralization at the Carter farm is similar to quartz vein mineralization in the Quantico Formation that occurs in a parallel structure approximately 600 m to the northwest and is marked by a greater than 6-km-long line of prospect pits and small mines dug in search of gold mineralization (Spears and Upchurch, 1997).

Some vein quartz in the Carter farm trenches, and pieces of residual vein quartz on the ground surface northeast of the trenches, have unusual sets of orthogonal planar fractures and white planar streaks. An oriented thin section of vein quartz from the south trench (north wall, 79 cm to the right and 82 cm down from reference nail n2) shows that macroscopically the quartz

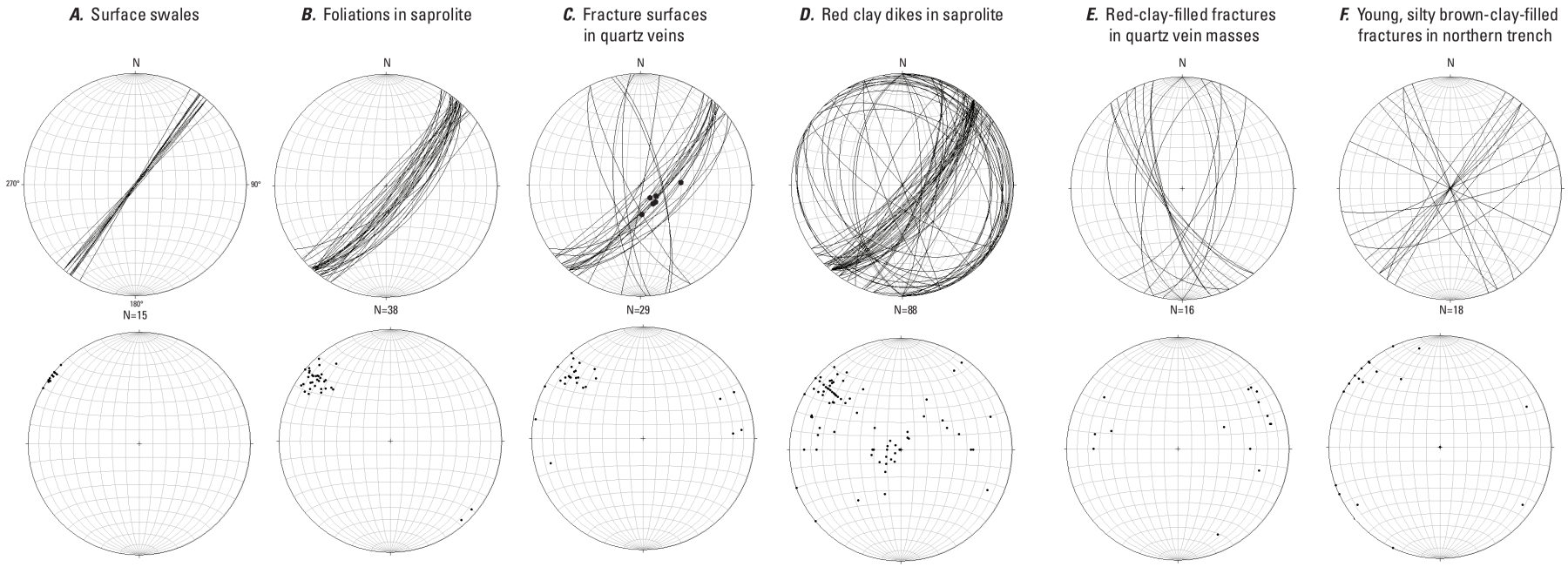

Figure 5. Equal-area, lower hemisphere stereonets showing the orientation of structural features measured at the surface and in exploratory trenches at Carter farm; the upper diagram shows great circles and the lower diagram shows poles to each plane. *A*, Strike of surface swales, plotted as vertical. *B*, Foliations in saprolite. *C*, Fracture surfaces in quartz veins; black dots are rakes of striations. *D*, Red clay dikes in saprolite. *E*, Red-clay-filled fractures in quartz vein masses. *F*, Young, silty brown clay-filled fractures observed in the north trench. Abbreviation: N, number of structural measurements.

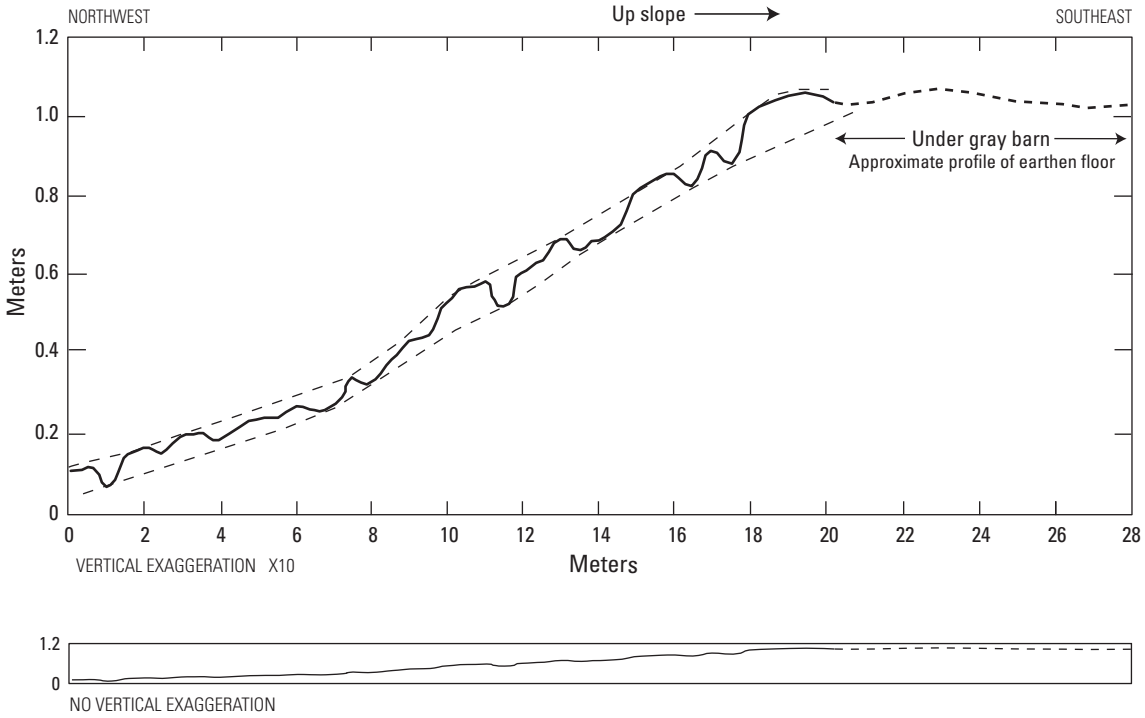

Figure 6. Profiles (looking north) of the ground surface across the deformed area at Carter farm at X10 vertical exaggeration and no vertical exaggeration (see fig. 4 for location and fig. 3 for photos). The profile was surveyed with a precision total station (Pentax); relative accuracy is sub-centimeter, both horizontal and vertical. The envelope that bounds the ridge crests and swale troughs along the X10 profile is shown as dashed lines.

is very light gray and has two orthogonal sets of planar fractures and white planar streaks less than 1 mm thick. In the oriented thin section, the principal set of planar fractures, or joints, and white planar streaks in the quartz vein is parallel to the vein wall (N5°W, 83°SW), and the orthogonal set of planar fractures and white planar streaks is perpendicular to the vein wall (N85°W, 90°). The quartz is almost entirely polycrystalline with some crystals greater than 1 centimeter across. Most quartz crystal boundaries have consertal intergrowth texture consistent with primary hydrothermal growth rather than granoblastic polygonal texture typical of metamorphic recrystallization. However, the quartz has strong undulatory extinction, indicating strain, and is highly fractured. Dynamically recrystallized quartz subgrains that lack undulatory extinction occur sparsely along and between fractures. Planar zones of fluid inclusions, interpreted as annealed fractures, correspond to white planar streaks observed macroscopically. Additionally, there are two main sets of closely spaced planar fractures and parallel fluid-inclusion planes that are orthogonal, with one set parallel to the vein wall and the other perpendicular to it. Two additional, oblique sets are more localized and widely spaced within the thin section. Fracture spacings vary, but are locally less than 1 mm apart. Fractures are mostly throughgoing across grain boundaries and appear to be mainly dilational without offset grain boundaries or other shear fabrics. The unusual geometry and abundance of planar fracture sets in quartz veins from the epicentral area of the 2011 M5.8 earthquake raises questions about possible relations to tectonics and seismicity.

Residuum

Overlying saprolite of the Quantico Formation is a layer of residuum that varies from about 20 cm to greater 1 m in thickness. This residuum is the B-soil horizon and is a red, massive, structureless clay that is a weathering residue of the Quantico Formation. The contact between residuum and saprolite is gradational and irregular, and is generally placed at the uppermost recognition of intact lithologic fabric. Remnants of quartz veins are easily identified in the residuum as the only non-clay-sized material. Generally, the remnant quartz extends from the parent vein in the saprolite as a trail of quartz fragments that decrease in number and size upward in the residuum. Typically, they are inclined to the northwest at an angle greater than the attitude of the parent vein. This suggests creep that is slowly moving residual material en mass down slope. Several of the remnant quartz veins in residuum extend to the base of the colluvium, but none extend into the colluvium.

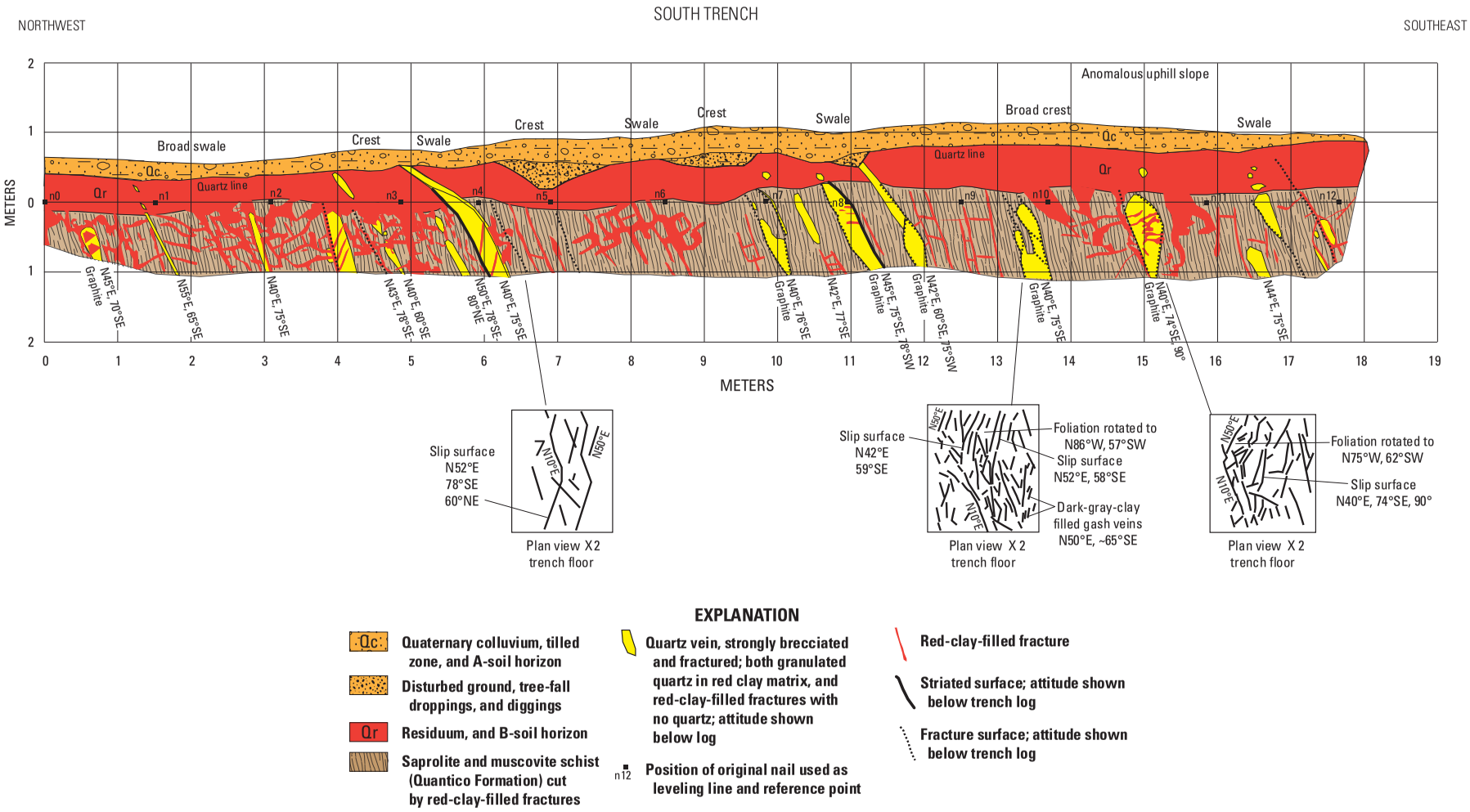

Figure 7. Diagrammatic log of the Carter farm south trench at no vertical exaggeration; view is towards the northeast; uphill is to the southeast. Elevation of the baseline (0 meters (m) on the figure) is approximately 450 feet above sea-level. Shown below the diagrammatic log are three plan views (X2 vertical exaggeration) displaying the structural fabric of the trench floor. For each set of orientation measurements shown, the first is strike; the second is dip; the third is rake (where applicable).

Red Clay Dikes of Residual Material in Saprolite

Extending downward from the massive residual layer into the upper saprolite are numerous tabular fractures filled with red clay similar to residuum. Widths of fractures vary from a few millimeters to several centimeters. The red-clay-filled fractures decrease in width and density downward. Orientations of the red-clay-filled fractures (fig. 5*D*) are both concordant (striking approximately N40°E, and dipping steeply to the southeast) and discordant to foliation (striking north to northwest, and dipping from a low-angle to horizontal). The orientations of the red-clay-filled fractures impart a brecciated pattern in the saprolite (figs. 7, 8 and 9*D*). Slickenside striations occur on the margins of several steeply dipping fractures that parallel foliation. Slickenside surfaces parallel foliation and striations are always oriented down dip ±10°.

Red-clay-filled fractures also cross cut the quartz veins, and in multiple places adjacent to the quartz veins, they contain angular fragments of quartz embedded in the clay. In other places, such as in a quartz vein at approximately the 4-m line in the south trench (fig. 7), en echelon northeast striking, steeply northwest dipping red-clay-filled fractures are prevalent.

The mechanism that led to formation of the red-clay-filled fractures is not fully understood. Two possibilities are (1) in situ formation, in which infiltrating groundwater altered material on fracture walls and this expanded outward, or (2) physically transported illuviation of clay-sized material downward from overlying residuum through the network of fractures. A transport mechanism is supported in places where red-clay-filled fractures cut across quartz veins, and many such examples of this is present in the trenches. Several red-clay-filled fractures cut both quartz veins and saprolite, therefore, we consider the clay in fractures to be most likely of transported origin. In addition to tabular fractures, red clay commonly fills the matrix between clasts in brecciated saprolite where the mechanism of formation is equivocal.

Brown Silty Clay Dikes in Residuum and Saprolite

Many thin (typically <2 cm) brown, silty clay-filled tabular fractures cut both residuum and saprolite in the north trench, but none extended into overlying colluvial layer (fig. 8). These brown clay fractures also cut the red-clay-filled fractures. A sample of the brown silty clay material was inspected for fossil pollen, but no pollen was found. Strike of the brown-clay-filled fractures is bimodal with a northeast trend parallel to foliation and a second trend that is generally to the north. Both trends are near vertical to steeply inclined eastward (fig. 5*F*). The brown-clay-filled fractures do not occur in the south trench, indicating that a localized process generated this type of fracturing.

Two additional occurrences of very similar brown, silty clay-filled fractures have been observed in the epicentral area of the August 2011, M5.8 earthquake. One was in an excavation for a new house approximately 7 km to the southwest of Carter farm at 10780 Shannon Hill Road. There, the Quantico Formation is saprolitized, but no quartz veins are present. Cutting the upper half of a Pleistocene(?) channelized gravel deposit (approximately 1 m thick), that rests directly on saprolite, are several 1 to 2 cm-thick, tabular, near vertical brown-clay-filled fractures trending both northeast and northwest. There were no fractures filled with clay in the saprolite, either below or outside of the channel margin, suggesting that whatever process formed the fractures, it was unique to the gravel deposit. The second occurrence of brown-clay-filled fractures similar to those at Carter farm is at Roundabout farm, which is located approximately 15 km to the west. Several exploratory trenches were excavated there and at one location tabular, brown-clay-filled fractures were observed extending upward from the margin of a quartz vein in saprolite through a sandy, clayey gravel deposit and terminating in the uppermost approximately 10-cm-thick tilled horizon (see Roundabout farm, trench number 1 in Burton and others, 2015). Optically stimulated luminescence (OSL) analyses from Burton and others (2015) suggests a late Pleistocene age for the gravel deposit, therefore, the brown-clay-filled fractures there are late Pleistocene or Holocene in age.

Colluvium

Colluvium overlies residuum in both trenches and the contact is a nearly continuous overlying layer of pebbles, separating transported material from underlying in situ material. Colluvium ranges from a few centimeters to about 0.5 m thick and contains an anthropogenic tilled horizon. The colluvial deposit is matrix supported and contains clasts that are typically subangular to subrounded, ranging from silt- and sand-sized material to small cobbles. Clasts are dominantly vein quartz and rarly quartzite.

The contact between colluvium and underlying residuum undulates in an irregular fashion, largely because of old tree-root depressions filled with gravely material that extend downward into residuum (figs. 7 and 8). There was no evidence of any vertical or horizontal shearing in the colluvium. Unconsolidated colluvium is less likely to develop brittle fabric like shearing.

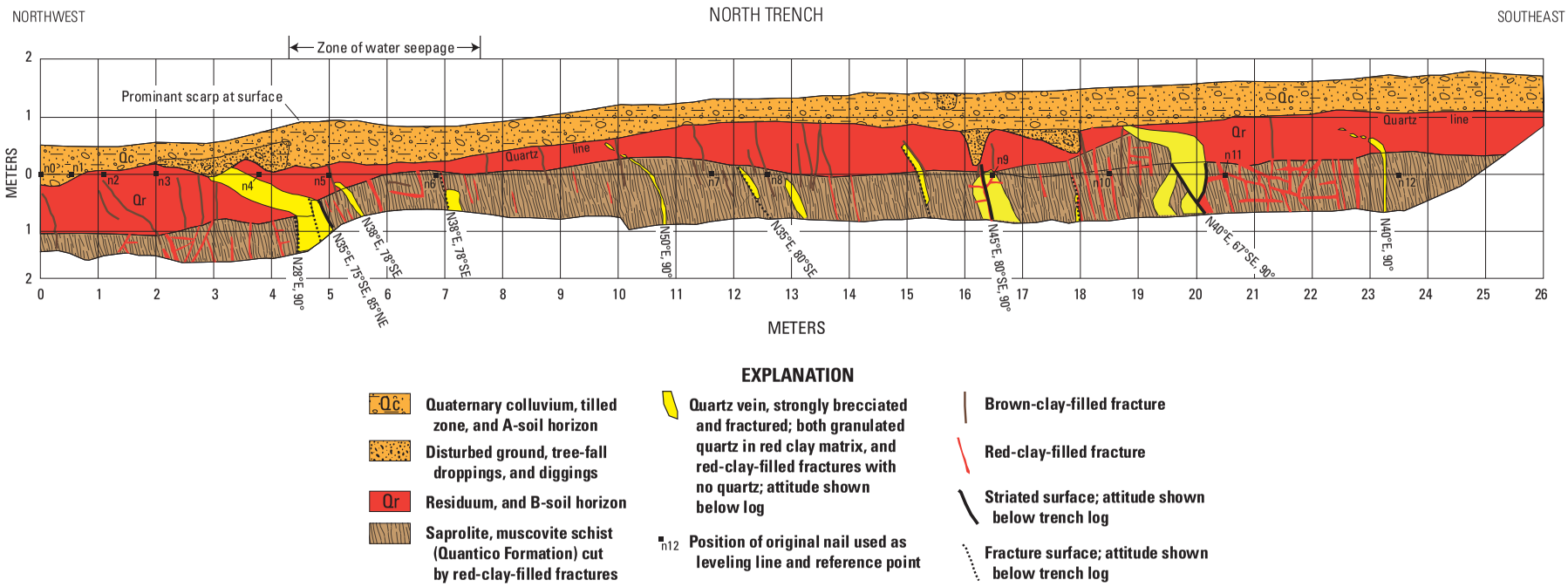

Figure 8. Diagrammatic log of the Carter farm north trench at no vertical exaggeration; view is towards the northeast. Elevation of the origin (0 meters (m) on the figure) is approximately 445 feet above sea-level. For each set of orientation measurements shown, the first is strike; the second is dip; the third is rake (where applicable).

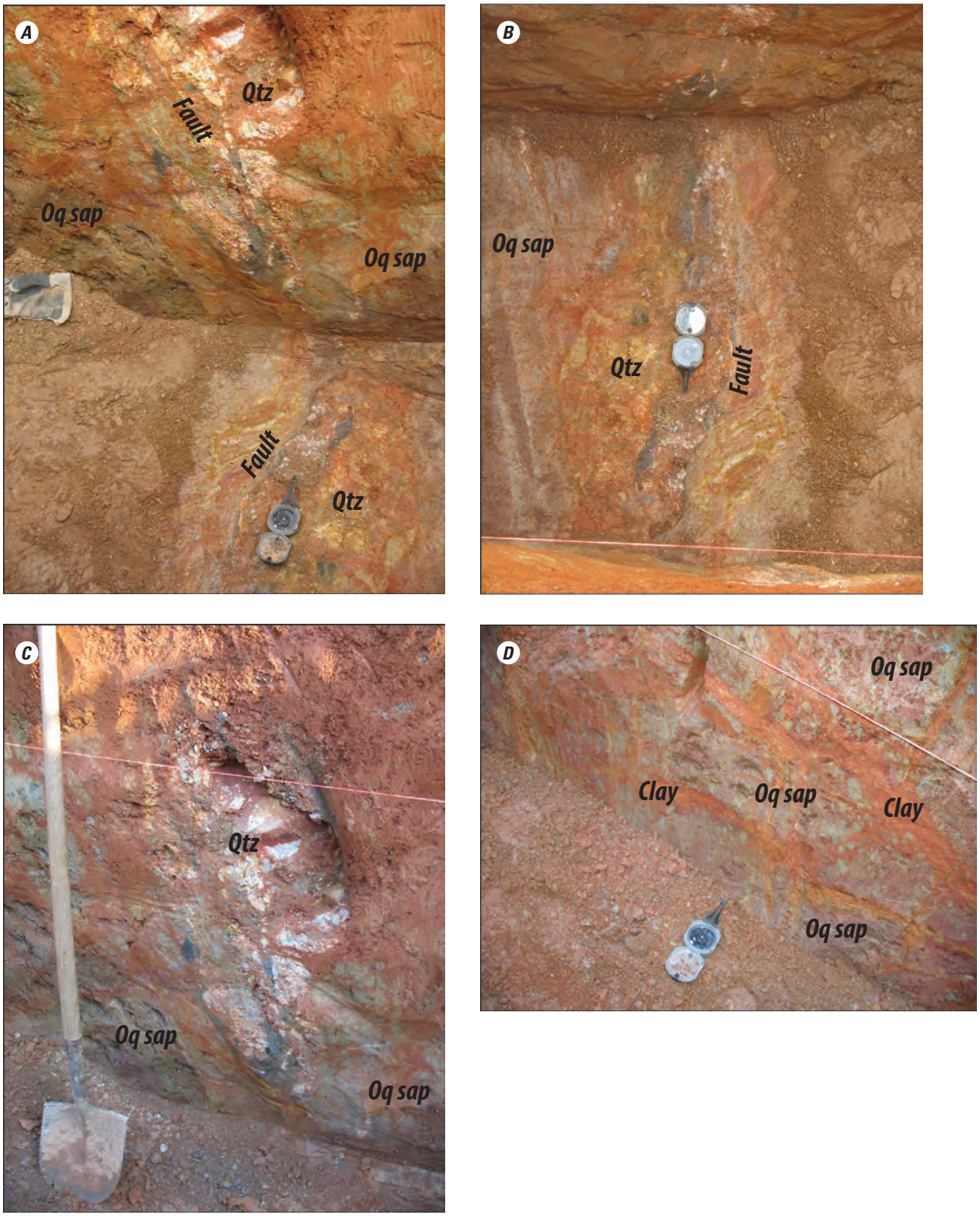

Figure 9. Photos showing structural features in the north and south trenches at Carter farm. *A*, Photo of a faulted quartz vein (Qtz) in saprolite schist of the Quantico Formation (Oq sap) in the south trench between the 13- and 14-meter (m) lines on figure 7; view is towards the northeast. *B*, Photo of the same fault as in *A* looking down at the trench floor and towards the southwest. *C*, Photo of a brecciated, sheared quartz vein at the 15-m line in the the south trench (fig. 7). *D*, Photo of fractured saprolite and low-angle red-clay-filled fractures (labeled as Clay) in the north trench between the 20- and 22-m lines on figure 8; view is towards the northeast. The Brunton compass is approximately 35 centimeters long; the string marks the level line in the trench.

Interpretations and Conclusions

Carter Farm Fault

The quartz veins in the trenches at Carter farm are interpreted as epithermal mineralization of open space that were created by brittle faulting between the Late Ordovician and Jurassic. Field data indicates multiples pulses of reactivated brittle deformation that post-dates vein formation. Quartz veins possess a brittle cataclastic fabric consisting of fracturing, brecciated, and granulated material through the entire depth of saprolite in both trenches (approximately 2.2 m depth). This brittle deformation defines the Carter farm fault. Kinematic indicators provided by near-dip-slip slickenside striations and subhorizontal shortening-directions indicate that the Carter farm fault is a southeast-dipping thrust. Because the occurrence of the Carter farm fault lies completely within the Quantico Formation (a saprolitized schist that lacks significant variation), estimates on the amount of displacement could not be determined.

The red-clay-filled fractures that cut saprolite and quartz veins cannot pre-date the modern B-horizon soil, thus, the age of these fractures is considered to be less than 2 million years, and probably less than 1 million years (Pavich and others, 1985; Pavich and others, 1989). Therefore, (1) the red-clay-filled fractures cutting quartz vein material, (2) the red clay fractures that contain angular fragments of quartz veins, and (3) the fabric of fractures in saprolitized Quantico Formation are also presumably Quaternary in age. This suggests Quaternary movement along the Carter farm fault. The slickenside striations along the fault are indicative of upward dip-slip (thrust) movement during the Quaternary. Assuming co-axial stress-strain relations, the implied maximum principal stress direction is similar to the 278° direction of the P-axis (strain) as determined for the August 23, 2011, earthquake (St. Louis University Earthquake Center, 2011).

There is no evidence of any brittle deformation, including shearing, in the colluvial layer that overlies the Carter farm fault. Although the actually age of colluvium is unknown, the lack of shearing would seem to preclude a late Holocene(?) seismicity of a magnitude great enough to cause brittle surface-rupturing along the Carter farm fault. However, the Carter farm fault is considered, one of the few known neotectonic structures in the epicentral area (Burton and others, 2015) because of its apparent Quaternary age.

Other examples of intra-formational faulting in the Quantico Formation have been recognized elsewhere. To the northeast in vicinity of Lake Anna (fig. 1), Mixon and others (2000) mapped two northeast-striking faults within the Quantico Formation. Both are mapped as offsetting contacts between differing metamorphic units and thus are post-metamorphic in age. We suggest that the Carter farm fault is related to, or is a continuation of, this faulting within the Quantico Formation. A prospected quartz-bearing structure to the northwest of the Carter farm fault is on a direct projection to the Sturgeon Creek fault (Mixon and others, 2000). We suggest that these two faults are part of the same deformation system. Mixon and others (2000) describes the Sturgeon Creek fault as a northeast-striking structure with sinistral displacement that offsets the contact between the Ta River Metamorphic Suite and the Quantico Formation, and curves southwestward into the axial region of the Quantico synclinorium. For a distance of over 60 km to northeast along the outcrop belt of the Quantico Formation, Mixon and others (2000) mapped several other northeast-striking faults parallel to the Sturgeon Creek fault. Several of these faults offset the Ta River-Quantico contact and are intra-formational in the Quantico Formation. Near Stafford, Va., Mixon and others (2000) describes the Dumfries fault zone of Newell and others (1976) as spatially coexisting closely with "the outcrop-subcrop belt of the relatively incompetent slates and phyllites of the Quantico Formation." Post-Cretaceous and post-Paleogene faulting has also been identified along the Dumfries fault zone (Newell and others, 1976; Mixon and others, 2000).

The subhorizontal red-clay-filled fractures are of interest because they suggest an upper dilation that strongly crosscuts the metamorphic fabric in the saprolite and is not readily explained by any hillslope-modifying surficial process, such as creep or mass failure. In some places, the steeply dipping (along foliation) red-clay-filled fractures cut subhorizontal red-clay-filled fractures. In other places, the opposite is true. And then there are some places where the intersection of the different sets shows no relative offset of one by the other, thus, suggesting that the different sets formed at the same time. Presumably, the steeply dipping set of red-clay-filled fractures helped facilitate upward dilation. At multiple locations, such as (1) the 20- to 22.5-m lines on the north trench log, (2) between the 1.5- and 2.5-m lines on south trench log, and (3) between the 12- and 13-m lines on the south trench log, the subhorizontal red-clay-filled fractures occur in en echelon patterns between adjacent steeply dipping fractured quartz veins. This possibly indicates that, under a subhorizontal compressive force, zones of subhorizontal dilation were created by differential slippage along the fractured quartz veins. This dilation would be along models of conjugate Reidel shears (R') at a high angle to the slip surface. Similar features occur along the Roundabout farm fault, approximately 10 km to the west of Carter farm (see discussion on "shear couples" and fig. 16 in Burton and others, 2015).

Studies of weathering profiles in the Virginia Piedmont by Pavich and others (1985) and Pavich and others (1989) did not recognize subhorizontal fractures as part of the typical regolith soil development. Alternately, hydrogeologists working in the

southeastern Piedmont of Virginia recognize that subhorizontal fractures at, or near, the bedrock-saprolite transition zone are relatively common and are generally regarded as conduits for enhanced groundwater flow (Melinda Chapman, U.S. Geological Survey, oral commun., 2013). A groundwater origin for the clay-filled fractures is unlikely because the red-clay-filled fractures diminish downward towards the saprolite-bedrock transition were they terminate. Furthermore, the permeability of the saprolite is very low, and there are no active groundwater conduits present today in the saprolite. Therefore, we favor a non-groundwater process as causing the subhorizontal red-clay-filled fractures and consider them a possible record of either tectonic or seismic activity in the Quaternary.

The brown-clay-filled fractures in the north trench are of particular interest because they are the youngest deformational feature and because similar fractures at Roundabout farm are thought to be of tectonic origin. Water seepage along quartz veins in the north trench occurred continuously during the period that it was open, but similar veins in the south trench were dry during the same period. This suggests a possible association between the brown-clay-filled fractures and groundwater. The topographic scarp on the west side of the north trench could be related to spring flow, or alternately it could have been excavated to utilize near-surface water.

Processes Responsible for Ground-Surface Deformation

The genesis of surface deformation described in this report is enigmatic and somewhat uncertain. The location of the surface deformation at Carter farm is located several kilometers from the surface projection of the causative fault (Quail fault zone) of the M5.8 earthquake (fig. 10), therefore, a primary genetic link is improbable. Creation of the surface features by gravitational slumping is disfavored as a possible causative process because of the low surface topographic gradient (<2°) and their morphology is inconsistent with landsliding. The lack of shearing in the colluvial layer suggests that secondary soil movement such as soil slides, soil avalanches, and soil slumps is not the cause of surface deformation at Carter farm. These features usually possess characteristic shear surfaces related to earthquakes (see table 12–1 in Yeats and others, 1997).

Three possible processes could account for the surface deformation, two of which are local tectonic in origin (within a couple kilometers of the Carter farm site) and one has a non-tectonic explanation, but none of these three are mutually exclusive. Our primary assumption is the surface features were formed in response to the 2011 M5.8 earthquake sequence as reported by multiple residents.

The first local tectonic model interprets the deformational features as the surface expression of minor, up-to-the southeast monoclinal flexuring, possibly accompanied by shearing at depth. The surveyed profile (fig. 6) across the features at Carter farm documents a broad northwest-facing monocline with approximately 1 m of up-to-southwest relief over a distance of about 20 m. The ridge and swale features occur on the northwest face of the monocline in an envelope about 10 cm thick, suggesting extensional flexuring. The monocline indicates up-to-southwest movement along the Carter farm fault, which dips at approximately 75° to the southwest. If this is the case, movement probably occurred as aseismic creep, because there are no recorded earthquake hypocenters down dip along the Carter farm fault (fig. 10). Groundwater concentrated along the Carter farm fault may have acted as a lubricant, facilitating possible aseismic movement. The broken quartz veins are conduits for groundwater movement, and the small blow-hole-like depressions suggest water venting along the structure.

The second local tectonic model interprets the monoclinal flexuring as the surface expression of very shallow movement associated with a northwest-southeast elongated cluster of aftershocks that occurred about 1 to 3 km to the southeast (figs. 2 and 10). Earthquakes defining this elongated cluster occurred early in the aftershock sequence and persisted for about three months (McNamara and others, 2014). The area of synform depressions are interpreted as uplifted abandoned stream valleys. Additionaly, the area of active stream piracy by Little River of the South Anna River tributary (fig. 2) lies between the elongated cluster of aftershocks and the Carter farm fault, suggesting a reoccurring genetic link consistent with long-term neotectonic uplift.

The non-tectonic model for formation of the ridge and swale features along the Carter farm fault associates differing responses between the rigid quartz veins and residuum/saprolite (with plastic characteristics) to seismically generated, ground-surface-waves (Rayleigh waves) radiating from a distant earthquake (the epicenter of the M5.8 earthquake). In this non-tectonic model (fig. 11), the broad arch over the Carter farm fault reflects an overall upward movement relative to the surrounding rocks. The ridges and swale features formed from extension over the arch coupled with differential upward movement between the quartz veins and the intervening saprolite. In this model, the individual “blocks” of quartz veins move towards the free-face ground surface while bulk dilation of the saprolite is accommodated by discrete dilation along the subhorizontal red-clay-filled fractures.

Far reaching ground motion induced by Rayleigh waves can be amplified in the near surface by soils (Gómez-Massó and others, 1983). Also, the counterclockwise motion of Rayleigh waves can produce an effect of vertical dilation and collapse (compression). Uenishi (2010) noted that on a free-face surface, vertical acceleration of particles is approximately 1.5 times

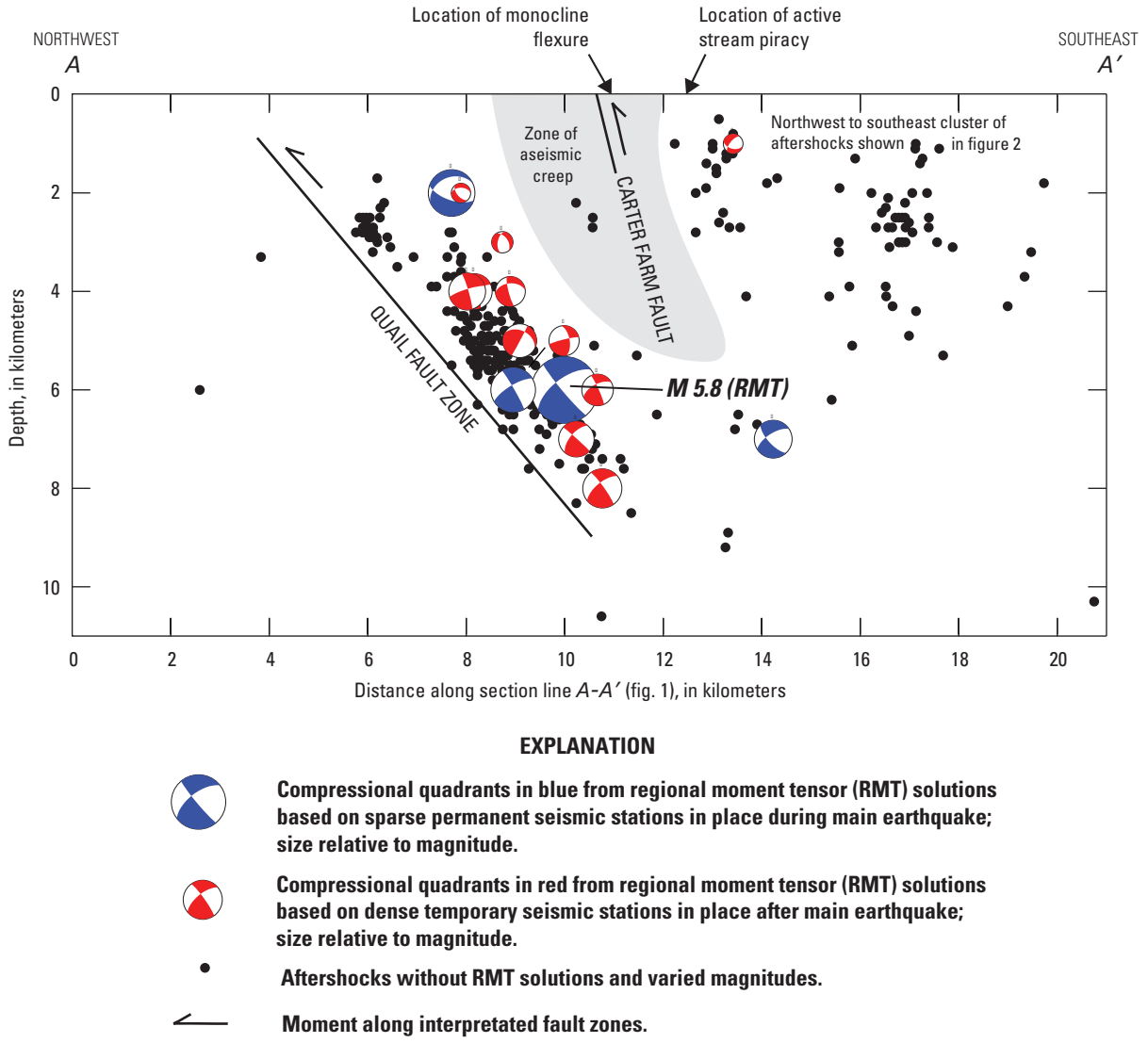

Figure 10. Northwest to southeast (left to right) profile along line *A–A′* in figure 1 that is through the epicentral area of the 2011 earthquake sequence; adapted from McNamara and others (2014) and Horton and others (2015). The Carter farm fault dips 75° to the southeast. Abbreviation: M, magnitude.

as large as horizontal acceleration. The strike line of the Carter farm fault, and outcrop belt of the Quantico Formation, trends directly towards the epicenter of the August 23, 2011, earthquake (fig. 1). Thus, one path of radiating seismic waves would travel directly along the fault from southwest to northeast. Property damage from the earthquake was also greater in this direction (Heller and Carter, 2015) further supporting that the non-tectonic model is a dominate mechanism.

In summary, cm-scale surface deformation occurred along the Carter farm fault during the 2011 M5.8 earthquake sequence. This deformation is comprised of parallel ridge and swales on the northwest face of a small monoclinal flexure. It is uncertain as whether this deformation is of tectonic or non-tectonic origin. The Carter farm fault is a brittle structure in the Quantico Formation that has a fabric indicative of episodic movement. This movement, and its associated fabric, had it youngest episode during the Quaternary as suggested by the involvement of material derived from the B-soil horizon.

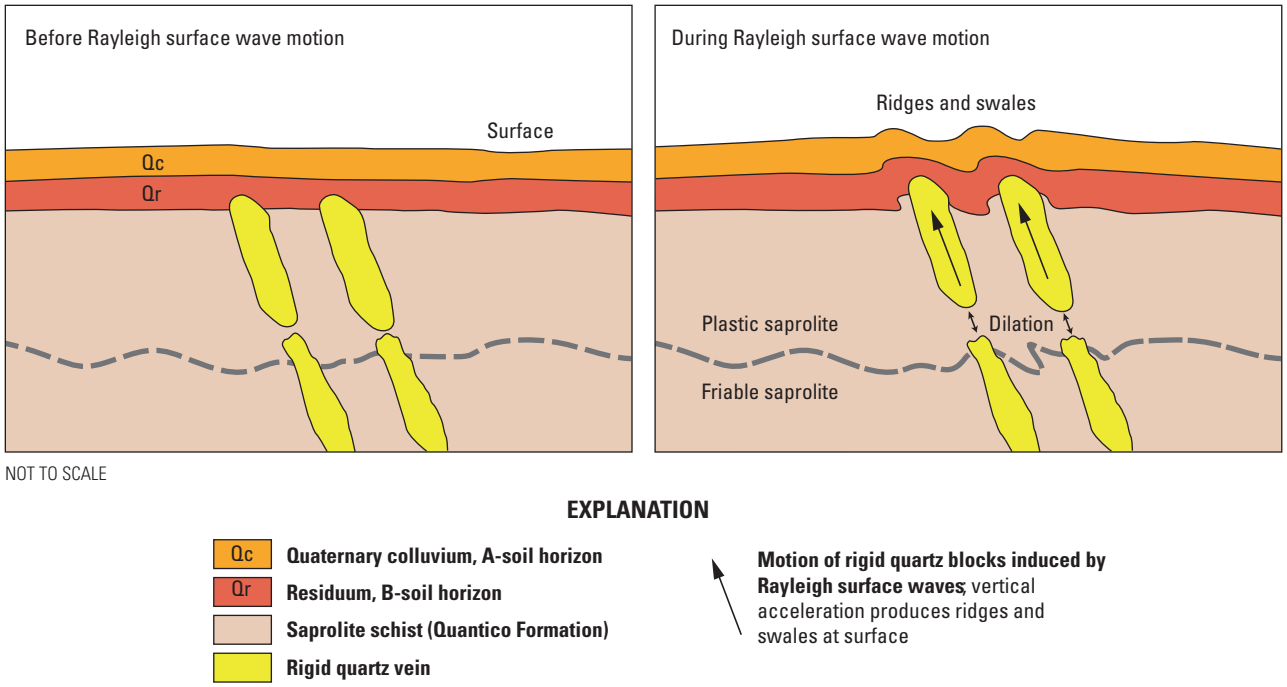

Figure 11. A schematic model showing a non-tectonic origin of ground-surface deformation at Carter farm. The left diagram is before Rayleigh surface wave motion. The right diagram is during Rayleigh surface wave motion. The Rayleigh surface waves travel away from the epicenter of the magnitude 5.8 earthquake, and along strike of the Carter farm fault (into the figure). The resulting ground surface deformation consists of linear ridges and swales across a broad arch over the fault.

Acknowledgments

We are grateful to the citizens of Louisa County, who were always very willing to allow us access to their property. Special thanks to Joe and Linda Carter for reporting the change to their farmyard following the August 23, 2011, earthquake and allowing us to further disturb the ground in our investigations. Also a special thanks to (retired) Colonel F.W. Billingsley for all the many times he has allowed geologists to trample his yard in order to inspect his fence, and for making sure that during construction of his new fence it was made straight and level ("gig line" military style), as this fence provides our best gage for evaluating what is otherwise very subtle ground-surface vertical deformation. We are also grateful to Arthur Schultz, William Burton, and David Shields (USGS) for their rigorous reviews and comments; along with Caryl Wipperfurth (USGS) for refining many of the illustrations.

References Cited

Burton, W.C., Harrison, R.W., Spears, D.B., Evans, N.H., and Mahan, Shannon, 2015, Geologic framework and evidence for neotectonism in the epicentral area of the 2011 Mineral, Virginia, earthquake, *in* Horton, J.W., Jr., Chapman, M.C., and Green, R.A., eds., The 2011 Mineral, Virginia, earthquake, and its significance for seismic hazards in Eastern North America: Geological Society of America Special Paper 509, p. 345–376, http://specialpapers.gsapubs.org/content/current.

Heller, M.J., and Carter, A.M., 2015, Residential property damage in the epicentral area of the Mineral, Virginia, earthquake of 23 August 2011, *in* Horton, J.W., Jr., Chapman, M.C., and Green, R.A., eds., The 2011 Mineral, Virginia, earthquake, and its significance for seismic hazards in Eastern North America: Geological Society of America Special Paper 509, p. 173–187, http://specialpapers.gsapubs.org/content/current.

Gómez-Massó, Alberto, Lysmer, John, Chen, Jian-Chu, and Seed, H.B., 1983, Soil-structure interaction with Rayleigh waves: Earthquake Engineering and Structural Dynamics, v. 11, p. 567–583, http://onlinelibrary.wiley.com/doi/10.1002/eqe.4290110409/pdf.

Horton, J.W., Jr., Aleinikoff, J.N., Drake, A.A., Jr., and Fanning, C.M., 2010, Ordovician volcanic-arc terrane in the central Appalachian Piedmont of Maryland and Virginia: SHRIMP U-Pb geochronology, field relations, and tectonic significance, *in* Tollo, R.P., Bartholomew, M.J., Hibbard, J.P., and Karabinos, P.M., eds., From Rodinia to Pangea; The lithotectonic record of the Appalachian region: Geological Society of America Memoir 206, p. 621–660, http://memoirs.gsapubs.org/content/206/621.full.pdf+html.

Horton, J.W., Jr., Shah, A.K., McNamara, D.E., Snyder, S.L., and Carter, A.M., 2015, Aftershocks illuminate the 2011 Mineral, Virginia, earthquake causative fault zone and nearby active faults, *in* Horton, J.W., Jr., Chapman, M.C., and Green, R.A., eds., The 2011 Mineral, Virginia, earthquake, and its significance for seismic hazards in eastern North America: Geological Society of America Special Paper 509, p. 253–271, http://specialpapers.gsapubs.org/content/509/253.

Marr, J.D., Jr., 2002, Geologic map of the western portion of the Richmond 30 x 60 minute quadrangle, Virginia: Virginia Department of Mines Minerals and Energy, Division of Mineral Resources Publication 165, scale 1:100,000, 1 sheet, http://www.dmme.virginia.gov/commercedocs/PUB_165.pdf.

McNamara, D.E., Benz, H.M., Herrmann, R.B., Bergman, E.A., Earle, Paul, Meltzer, Anne, Withers, Mitch, and Chapman, M.C., 2014, The M_w 5.8 Mineral, Virginia, earthquake of August, 2011 and aftershock sequence; Constraints on earthquake source parameters and fault geometry: Bulletin of the Seismological Society of America, v. 104, no. 1, p. 40–54, http://www.bssaonline.org/content/104/1.toc.

Mixon, R.B., Pavides, Louis, Powars, D.S., Froelich, A.J., Weems, R.E., Schindler, J.S., Newell, W.L., Edwards, L.E., and Ward, L.W., 2000, Geologic map of the Fredericksburg 30' x 60' quadrangle, Virginia and Maryland: U.S. Geological Survey Geologic Investigations Series Map I–2607, 34-p. pamphlet, 2 pls., scale 1:100,000. [Also available at http://pubs.er.usgs.gov/publication/i2607.]

Newell, W.L., Prowell, D.C., and Mixon, R.B., 1976, Detailed investigation of a Coastal Plain-Piedmont fault contact in northeastern Virginia: U.S. Geological Survey Open-File Report 76–329, 14 p. [Also available at http://pubs.er.usgs.gov/publication/ofr76329.]

Pavich , M.J., Leo, G.W., Obermeier, S.F., and Estabrook, J.R., 1989, Investigations of the characteristics, origin, and residence time of the upland residual mantle of the Piedmont of Fairfax County, Virginia: U.S. Geological Survey Professional Paper 1352, 58 p., 3 pls. [Also available at http://pubs.er.usgs.gov/publication/pp1352.]

Pavich, M.J., Brown, Louis, Valette-Silver, J.N., Klein, Jeffrey, and Middleton, Roy, 1985, ^{10}Be analysis of a Quaternary weathering profile in the Virginia Piedmont: Geology, v. 13, no. 1, p. 39–41, http://geology.geoscienceworld.org/content/13/1/39.full.pdf+html?sid=c518af62-ea56-4ae4-936a-d63f6992a181.

Pavlides, Louis, Pojeta, John, Jr., Gordon, Mackenzie, Jr., Parsley, R.L., and Bobyarchick, A.R., 1980, New evidence for the age of the Quantico Formation in Virginia: Geology, v. 8, no. 6, p. 286–290, http://geology.geoscienceworld.org/content/8/6/286.full.pdf+html?sid=410e9bc3-3d4a-4c22-96dc-ba337838dc82.

St. Louis University Earthquake Center, 2011, August 23, 2011 Virginia: Saint Louis University Earthquake Center Web page, accessed January 15, 2012, at http://www.eas.slu.edu/eqc/eqc20110823.html.

Spears, D.B., and Upchurch, M.L., 1997, Metallic mines, prospects, and occurrences in the gold-pyrite belt of Virginia: Virginia Department of Mines Minerals and Energy, Virginia Division of Mineral Resources Publication 147, 73 p., https://www.dmme.virginia.gov/commerce/ProductDetails.aspx?productID=1281.

Uenishi, Koji, 2010, On a possible role of Rayleigh surface waves in dynamic slope failures: International Journal of Geomechanics, v. 10, no. 4, p. 153–160, http://ascelibrary.org/doi/pdf/10.1061/%28ASCE%29GM.1943-5622.0000057.

Yeats, R.S., Sieh, Kerry, and Allen, C.R., 1997, The geology of earthquakes: New York and Oxford, Oxford University Press, 576 p.

For more information concerning this publication, contact:
Eastern Geology and Paleoclimate Science Center
U.S. Geological Survey
926A National Center
12201 Sunrise Valley Drive
Reston, VA 20192

http://geology.er.usgs.gov/egpsc/

Publishing support provided by the
Reston Publishing Service Center

Editing by David A. Shields

Illustrations by Caryl Wipperfurth

Layout by Jeannette M. Foltz

Web support by Angela E. Hall

ISSN 2331-1258 (online)
http://dx.doi.org/10.3133/ofr20161134